PHYSICAL REVIEW LETTERS

Chirping of an Optical Transition by an Ultrafast Acoustic Soliton Train in a Semiconductor Quantum Well

A. V. Scherbakov,[1,2] P. J. S. van Capel,[3,*] A. V. Akimov,[1,2] J. I. Dijkhuis,[3] D. R. Yakovlev,[1,2]
T. Berstermann,[1] and M. Bayer[1]

[1]*Experimentelle Physik II, University of Dortmund, D-44221 Dortmund, Germany*
[2]*A. F. Ioffe Physico-Technical Institute, 194021 St. Petersburg, Russia*
[3]*Debye Institute, Department of Physics and Astronomy, University of Utrecht, P.O. Box 80000, 3508 TA Utrecht, The Netherlands*
(Received 22 December 2006; published 1 August 2007)

Acoustic solitons formed during the propagation of a picosecond strain pulse in a GaAs crystal with a ZnSe/ZnMgSSe quantum well on top lead to exciton resonance energy shifts of up to 10 meV, and ultrafast frequency modulation, i.e., chirping, of the exciton transition. The effects are well described by a theoretical analysis based on the Korteweg−de Vries equation and accounting for the properties of the excitons in the quantum well.

Nonlinear elastic properties of solids result in the striking phenomenon of the transformation of a coherent strain wave packet to a train of ultrashort acoustic solitons. Such solitons propagate strongly directionally through the crystal with a velocity slightly above the velocity of longitudinal sound, introducing at each momentary position a "nanoearthquake." The first experimental observation of an acoustic soliton by Hao and Maris in 2001 [1] was followed by detailed studies [2–6] that have shown that a single soliton pulse can occupy a space as small as a few nanometers, corresponding to durations as short as a few hundred femtoseconds, and may reach strain amplitudes exceeding 10^{-3}. These spatial and temporal characteristics of acoustic solitons are close to the typical sizes of nanostructures (quantum wells, wires, and dots) and relaxation times of their electronic excitations, respectively, which were studied intensively during the last decades. Thus the discovery of acoustic solitons may open up a new research field in solid state physics where subpicosecond and nanometer control of the optical response of nanostructures is achieved by acoustic solitons without generation of carriers.

In this Letter we present the first experimental and theoretical study of ultrafast frequency modulation (chirping) of an exciton resonance in a semiconductor quantum well (QW) by an acoustic soliton train. When the QW is hit by the "nanoearthquake," the exciton experiences an energy shift as high as 10 meV on a picosecond time scale, as is demonstrated via its optical response. The theoretical analysis of this soliton-induced effect takes into account the finite QW width and the exciton coherence time. Excellent agreement between experiment and theory is reached, which paves the way for a new class of quantitative ultrafast acoustic experiments in semiconductor nanostructures.

The idea and scheme of the experiment are shown in Fig. 1(a). The sample used was a (001)-oriented GaAs slab with a thickness $l_0 \sim 0.1$ mm. The heterostructure

deposited by MBE on the front side of the slab was a ZnSe QW with a width $a = 8$ nm embedded between $Zn_{0.89}Mg_{0.11}S_{0.18}Se_{0.82}$ barriers. The details of the fabrication and the properties of the structure can be found elsewhere [7]. A 113-nm thick Al film was deposited on the back side of the GaAs slab. This metal film acts as an optoelastic transducer upon excitation by a short laser pulse and injects a strain pulse into the GaAs slab [8,9]. In our experiments the sample was immersed in liquid helium ($T_0 = 1.8$ K), and the Al film was excited by 200-fs pulses from an amplified Ti-sapphire laser (wavelength 800 nm) with a repetition rate of 250 kHz. This pump beam was focused to a 100-μm FWHM spot on
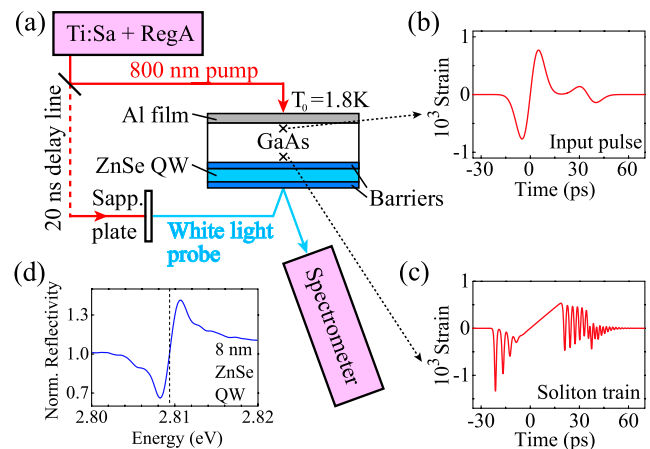

FIG. 1 (color online). (a) Experimental scheme. (b) Calculated strain pulse as initially generated in the metal film for excitation density $W = 10$ mJ/cm², and (c) its transformation to a soliton train after propagation through 0.1 mm of GaAs. The time in (b) is shifted toward that in (c) by the sample traversal time t_0. (d) The measured reflectivity spectrum of the ZnSe QW, normalized to the off-resonance background. The vertical dashed line in (d) shows the energy position of the heavy-hole exciton resonance.

the film, creating energy densities W up to 10 mJ/cm² per pulse. The temporal evolution of the injected strain pulse [Fig. 1(b)] was calculated using the known methods of ultrafast acoustics [8,9] and coincides with results from direct conventional pump-probe measurements [10]. In our experiments we have a nearly symmetric bipolar strain wave packet as an input pulse, which can be modeled to a good degree of accuracy by a Gaussian derivative with a typical width ~7 ps, and strain amplitudes reaching 8×10^{-4} in GaAs for the highest pump intensity. The temporal and spatial evolution of the strain pulse $\varepsilon_W(t, x)$ (where x is the distance from the Al film) depends on W and on the linear and nonlinear elastic properties of the crystal and can be calculated by numerically solving the Korteweg–de Vries equation [1–6]. At low pump excitation density ($W < 1$ mJ/cm²), the injected strain pulse propagates linearly through the GaAs slab with the velocity of longitudinal sound ($s_{\text{GaAs}} = 4.8 \times 10^3$ m/s) and reaches the ZnSe/ZnMgSSe heterostructure at a time $t_0 \sim l_0/s_{\text{GaAs}} \sim$ 20 ns without any sizable distortion. At excitation densities $W > 1$ mJ/cm², however, nonlinear elastic effects start to play a role and the injected strain pulse transforms into a more complicated waveform. At medium fluences 1–3 mJ/cm², the wave develops into a shock wave—an intermediate stage in the soliton development. Finally, above 3 mJ/cm², dispersion makes the supersonic compressive strain develop into a train of short soliton pulses. Figure 1(c) shows an example trace for $\varepsilon_W(t, x)$, calculated for our experimental conditions, $W = 10$ mJ/cm² and $x = l_0$. The most salient features are the development of acoustic frequencies in the THz range, and the formation of supersonic solitons at the front.

The effect of the soliton pulses on the optical response of the QW was studied using ultrafast optical spectroscopy. For this, a probe beam was split from the laser beam, passed through a sapphire plate to generate femtosecond white light pulses, and given an optical delay of 20 ns, corresponding to the travel time of the longitudinal strain pulse through the crystal slab. The probe beam was focused on the front side of the slab to a spot less than 50-μm diameter exactly opposite to the pump spot [Fig. 1(a)]. The specularly reflected probe beam was collected and analyzed by a spectrometer and CCD camera with the readout synchronized with the scanning optical delay line in the pump beam. The overall time resolution of the setup was better than 300 fs.

Figure 1(d) shows the reflectivity spectrum in the absence of a pump pulse in the energy range of the heavy-hole exciton resonance in the QW, which was earlier studied in detail for similar samples [7]. The exact shape of the reflectivity spectrum is determined by the thickness of the top barrier layer [11]. For our sample, the reflectivity normalized to the off-resonant background can be described by the equation

$$r(E) = 1 + A_0 \frac{E - E_0}{\Gamma^2 + (E - E_0)^2}, \quad (1)$$

with A_0 a constant, $E_0 = 2.809$ eV the static position of the exciton line at this temperature, and $\Gamma \sim 1$ meV the measured resonance width, limited by the instrumental resolution and inhomogeneous broadening.

The main experimental task of this work was to measure the ultrafast optical response when the soliton train hits the QW. The results for three values of W are shown in Fig. 2 as spectral-temporal contour plots. The color and tone in each panel of Fig. 2 are a measure of the time-dependent reflected spectral intensity normalized to the off-resonant value. Animations that show the time evolution of experimental spectra are also available [12]. The value $t = 0$ corresponds to the arrival time t_0 of the center of the initial bipolar wave packet [Fig. 1(b)] at the QW. Times $t < -25$ ps and $t > 100$ ps correspond to the situation prior to the arrival of the strain wave packet at and after full passage of the heterostructure, respectively. No temporal modulation is observed and the reflectivity spectrum is equal to the one in the absence of strain, shown in the insets of Fig. 2 by a dashed line.

In the time interval $-25 < t < 100$ ps, however, the measurements show strong responses that depend on the pump excitation density W. In the linear regime [$W < 1$ mJ/cm², Fig. 2(a)] the optical response essentially tracks the temporal evolution of the exciton resonance, as shown earlier in a GaAs/AlGaAs QW for strain amplitudes less than 10^{-4} [13]. The important point here is that the exciton resonance does not change shape but simply shifts to different energies [compare solid and dashed lines in the inset of Fig. 2(a)]. Therefore, the strain-induced shift of the exciton resonance $\Delta E(t)$ can be approximated by $\Delta E(t) = c\varepsilon_{\text{QW}}(t)$, where c is the deformation potential. The time-dependent strain in the QW $\varepsilon_{\text{QW}}(t) = \varepsilon_0(t) - \varepsilon_0(t - t_r)$ consists of the sum of the pulse $\varepsilon_0(t)$ incident from the GaAs slab (taking into account impedance mismatch), and its reflection $-\varepsilon_0(t - t_r)$ from the sample–liquid-helium interface, arriving a time $t_r = 2l_r/\bar{s}$ later ($l_r = 50$ nm is the distance from the QW to the surface, and $\bar{s} = 4$ km/s is the mean longitudinal sound velocity in the ZnSe/ZnMgSSe heterostructure [14]); both are indicated in Fig. 2(a). The minus sign in the reflected wave is due to the phase jump of π at a free surface.

Huge changes in the time-resolved reflectivity spectra are observed for higher W [Figs. 2(b) and 2(c)]: (i) sharp features in the temporal signal appear, (ii) the leading edge of the detected signal shifts to earlier times with the increase of W, (iii) the spectrum broadens strongly [inset Fig. 2(b)], and (iv) doublet structures appear at certain values of time [inset Fig. 2(c)]. Features (i) and (ii) point to ultrafast solitons arriving at the QW. From the simulations we know that the soliton pulses may become shorter than 1 ps [see Fig. 1(c)], explaining the sharp features in the temporal evolution of the detected signal at high W. Furthermore, the soliton velocity is supersonic, which results in the early arrival of the front of the strain wave packet, as observed [1,4,6].
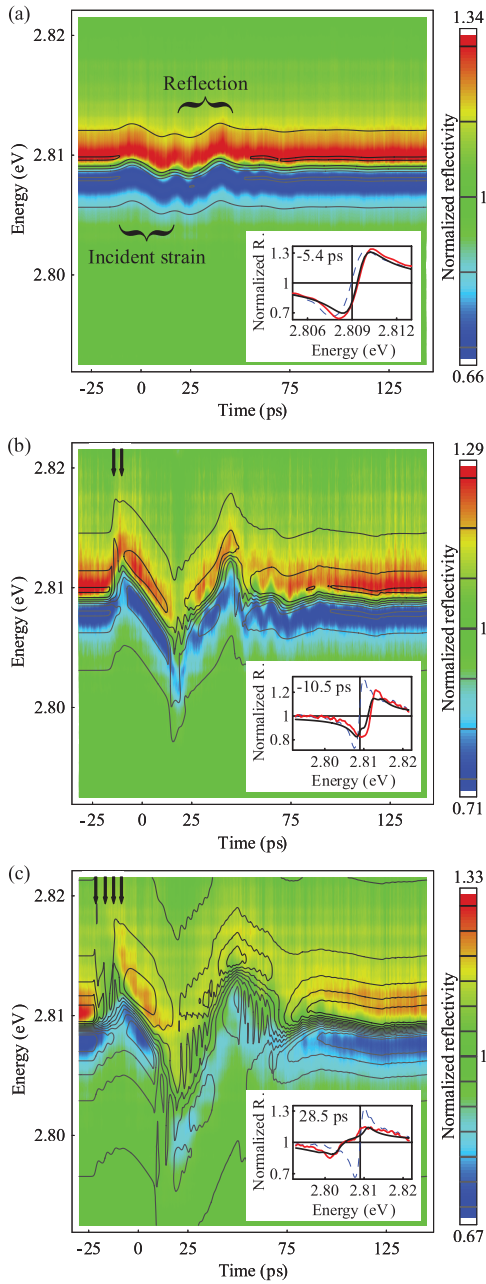
FIG. 2 (color). Spectral-temporal contour plots of the reflectivity normalized to the off-resonance background, measured for pump fluences of (a) 1 mJ/cm², (b) 5.1 mJ/cm², and (c) 10.2 mJ/cm². Black lines are calculated contours of equal reflectance changes for corresponding pump fluences. Insets show the spectral profiles of reflectivity: blue dashed line is the stationary spectrum, red and black lines are, respectively, the measured and calculated spectra at the specified time, for the corresponding fluence. Black arrows in (b) and (c) indicate the arrival time of individual solitons at the QW center.

To understand the optical response on a quantitative level, we calculate the temporal evolution $\Delta E(t)$ of the exciton resonance upon passage of a soliton train. We use GaAs material parameters and numerically calculate the wave shape $\varepsilon_{QW}^W(t, x)$ at the QW as input. Here, we include

reflections at the barrier layer/GaAs interface, and the fact that the QW experiences the strain of both the incident and reflected pulse. Because of the small distance between the QW and the surface, the temporal shapes of the incident and reflected strain pulses are taken identical except for the phase jump. In the soliton regime the spatial variations become so rapid that we cannot consider the QW as an infinitely narrow object. To analyze this we use the approximation of infinitely high barriers to find the electron wave function $\varphi(x') = \sqrt{2/a} \cos(\pi x'/a)$ ($x' = 0$ at the center of the QW). The finite size restricts the time resolution to $a/\bar{s} \sim 2$ ps, the travel time through the QW, and limits the sensitivity for very short soliton pulses, where the energy is concentrated mostly in the high-frequency components. Assuming that the strain does not change the potential profile of the QW significantly, perturbation theory gives the energy shift of the exciton resonance in the QW in the presence of the strain pulse as

$$\Delta E(t) = c \int_{-a/2}^{a/2} |\varphi(x')|^2 \varepsilon_{QW}^W(t, x')dx'. \qquad (2)$$

Here we note that Eq. (2) is reminiscent of the equation of matrix elements for the exciton-phonon interaction in a QW [15] that indeed shows a cutoff for high-frequency phonons.

The interaction of the probe light with the exciton system is inherently not instantaneous but takes the exciton coherence time T_e, which in high-quality QWs at low temperatures is close to twice the value of the radiative exciton lifetime [16] and much longer than the duration of the probe pulse and the strain soliton pulses. Thus a spectral broadening and shift of the exciton resonance are induced by the strain profile arriving at the QW up to a coherence time T_e *after* the incident probe pulse. To compute this, we approximate the transient reflectivity spectrum $R(E, t)$ as a convolution:

$$R(E, t) = \frac{1}{T_e} \int_t^\infty r[E - \Delta E(\tau)] \exp\left(-\frac{\tau - t}{T_e}\right)d\tau, \qquad (3)$$

where $r(E)$ and $\Delta E(\tau)$ are given by Eqs. (1) and (2), respectively.

To evaluate $R(E, t)$, we have developed an automated fitting procedure in which the width and height of the input wave and the coherence time T_e are the free parameters. The obtained input wave width [Fig. 1(b)] and amplitude $(7.5 \pm 0.2) \times 10^{-5}W$ were in good agreement with the values obtained in the pump-probe measurements mentioned before. The best agreement for the values of the shift is obtained for $c = -8$ eV. Further, we find $T_e = 4.6 \pm 1.3$ ps, close to the measured dephasing time of excitons in similar QWs [17]. The results of the numerical calculations for three values of W are shown in Figs. 2(a)–2(c) as solid contour lines of equal reflectivity. Good agreement between the experiment and simulations is observed. The sharpening of the leading edges at elevated W signifies the formation of ultrashort strain pulses, i.e.,

solitons, indicated by arrows in Figs. 2(b) and 2(c). The arrival time of the solitons decreases with the increase of W, as correctly described by the simulations. The inset of Fig. 2(b) shows a typical chirped spectrum at the time of passage of a soliton, which has clearly induced both a shift and significant broadening.

The simulations and experiments at the highest energy density show individual soliton pulses, which, however, seem to be largely washed out. The passage of incident and reflected solitons leads to strong spectral broadening over a large range of times, visible as an increase in green areas in Fig. 2(c). The reasons for this are that both the duration of individual soliton pulses and the time separation between different soliton pulses are shorter than T_e. Thus as soon as the soliton train arrives, the exciton resonance is driven several times back and forth during its coherence time T_e. We checked with simulations that this chirping has a fundamentally different character than when assuming Gaussian temporal broadening (e.g., present due to the nanometer roughness of the Al film surface), and is absent when $T_e = 0$, signifying the importance of the finite coherence time in picosecond exciton manipulation.

An even more elucidating example is presented in the inset of Fig. 2(c), which shows a clear doublet structure that can be observed around $t = 28$ ps. We can explain this by the tensile part of the incident wave, shown in Fig. 1(b). Here, a dispersive tail develops of both high frequency and high amplitude [Fig. 1(c)]. Within time T_e, the excitons are swept in energy over several meV a couple of times. One can qualitatively understand the origin of the doublet by making the analogy with a pendulum, which spends most of the time in its extreme positions.

At high W both experiment and theory show that $\Delta E(t)$ reaches 10 meV [Fig. 2(c)] at $t = 20$ ps and reveal that the reflected pulse induces higher excursions relative to the incident one. This experimental observation, which is absent for low W, is due to the circumstance that the first soliton pulse reflected from the surface and the tensile part of the incident pulse train meet in the QW and interfere constructively. All experimental results presented in Fig. 2 show minor amplitude oscillations with a period $\sim$10 ps after passage of the incident pulse which are not present in the simulated curves, and are not understood yet.

The presented work uses the QW as the archetypal object of semiconductor nanostructures. The observed constructive interference between incident and reflected strain pulses is analogous to coherent strain control [18] and realizes manipulation of nanostructures by acoustic soliton pulses. The soliton-induced effects in more sophisticated nanostructures (e.g., tunneling devices, shallow QWs, quantum wires, dots, and molecules), where the adiabatic approximation for electron and lattice systems is not valid anymore, may lead to the discovery of new and ultrafast phenomena at *constant* carrier densities. The experiments and theoretical analysis show that the effect of acoustic

solitons on the electronic state may be used as an ultrafast method for modulating the optical response in nanostructures. The large value of the energy resonance shift may become a basis for picosecond control of emission from nanophotonic devices (semiconductor microcavities, 2D arrays, etc.) and other switching principles in nanoelectronic and photonic devices.

*p.j.s.vancapel@phys.uu.nl

[1] H. Y. Hao and H. J. Maris, Phys. Rev. B **64**, 064302 (2001).
[2] O. L. Muskens and J. I. Dijkhuis, Phys. Rev. Lett. **89**, 285504 (2002).
[3] O. L. Muskens, A. V. Akimov, and J. I. Dijkhuis, Phys. Rev. Lett. **92**, 035503 (2004).
[4] B. C. Daly, T. B. Norris, J. Chen, and J. B. Khurgin, Phys. Rev. B **70**, 214307 (2004).
[5] O. L. Muskens and J. I. Dijkhuis, Phys. Rev. B **71**, 104304 (2005).
[6] E. Péronne and B. Perrin, Ultrasonics **44**, e1203 (2006).
[7] G. V. Astakhov et al., Phys. Rev. B **65**, 165335 (2002).
[8] G. Tas and H. J. Maris, Phys. Rev. B **49**, 15 046 (1994).
[9] T. Saito, O. Matsuda, and O. B. Wright, Phys. Rev. B **67**, 205421 (2003).
[10] P. J. S. van Capel and J. I. Dijkhuis, Appl. Phys. Lett. **88**, 151910 (2006).
[11] E. L. Ivchenko et al., Sov. Phys. Semicond. **22**, 495 (1988).
[12] See EPAPS Document No. E-PRLTAO-99-013732 for animations showing the shape of the measured spectrum as a function of time, for the three powers shown in Figs. 2(a)–2(c). For more information on EPAPS, see http://www.aip.org/pubservs/epaps.html.
[13] A. V. Akimov, A. V. Scherbakov, D. R. Yakovlev, C. T. Foxon, and M. Bayer, Phys. Rev. Lett. **97**, 037401 (2006).
[14] B. H. Lee, J. Appl. Phys. **41**, 2984 (1970).
[15] A. V. Akimov, in *Electron-Phonon Interactions in Low-Dimensional Structures*, edited by L. J. Challis (Oxford University Press, Oxford, 2003), p. 239.
[16] E. J. Mayer, N. T. Pelekanos, J. Kuhl, N. Magnea, and H. Mariette, Phys. Rev. B **51**, 17 263 (1995).
[17] H. P. Wagner, A. Schätz, R. Maier, W. Langbein, and J. M. Hvam, Phys. Rev. B **56**, 12 581 (1997).
[18] Ü. Özgür, C.-W. Lee, and H. O. Everitt, Phys. Rev. Lett. **86**, 5604 (2001).